COMPARING THE RETRIEVAL OF CHLOROPHYLL FLUORESCENCE FROM TWO AIRBORNE HYPERSPECTRAL IMAGERS WITH DIFFERENT SPECTRAL RESOLUTIONS FOR PLANT PHENOTYPING STUDIES

A. Belwalkar[1], T. Poblete[2], A. Longmire[2], A. Hornero[3,4], P.J. Zarco-Tejada[1,2,3]

[1]Department of Infrastructure Engineering, Faculty of Engineering and Information Technology (FEIT), The University of Melbourne, Melbourne, Victoria, Australia
[2]School of Agriculture and Food, Faculty of Veterinary and Agricultural Sciences (FVAS), The University of Melbourne, Melbourne, Victoria, Australia
[3]Instituto de Agricultura Sostenible (IAS), Consejo Superior de Investigaciones Científicas (CSIC), Alameda del Obispo s/n, 14004 Córdoba, Spain
[4]Department of Geography, Swansea University, SA2 8PP Swansea, United Kingdom

IGARSS 2021 - 2021 IEEE International Geoscience and Remote Sensing Symposium | 978-1-6654-0369-6/21/$31.00 ©2021 IEEE | DOI: 10.1109/IGARSS47720.2021.9553265

ABSTRACT

Several studies have demonstrated the influence of the spectral resolution (SR) on the retrieval of solar-induced chlorophyll fluorescence (SIF) from ground-based sensors with different spectral configurations. However, research studying the implications of the SR of airborne hyperspectral imagers on the retrieved SIF is lacking, and its interpretation is critical for precision agriculture, plant stress detection and phenotyping studies. This work investigates the effects of SR on SIF performance through the Fraunhofer Line Depth (FLD) principle at the O_2-A absorption feature (760.4 nm) using two airborne hyperspectral imagers with different spectral characteristics. A sub-nanometer hyperspectral imager with 0.1-0.2 nm full-width at half-maximum (FWHM) resolution and a broader-band hyperspectral imager of 5.8 nm FWHM were flown in tandem. The campaigns were conducted over a winter wheat field with randomized experimental design, with plots receiving different nitrogen rates to ensure SIF variability. Results showed a bias on the SIF levels quantified by both airborne imagers (RMSE=3.7 $mW/m^2/nm/sr$), but a strong relationship between both sensors at the O_2-A absorption feature (R^2=0.84, $p<0.001$). Results confirm the utility of hyperspectral imagers ca. 5 nm FWHM resolution for stress detection and plant phenotyping where assessing the relative variability of SIF across experimental plots is sought.

Index Terms— Airborne, hyperspectral, SIF, FLD, chlorophyll fluorescence, plant phenotyping

1. INTRODUCTION

The energy dissipation pathway by the photosynthetic apparatus in the form of SIF serves as a direct indicator of the physiological state of plants and can assist understanding of plant functioning, crop performance and the early symptoms of biotic and abiotic stress. Over the last two decades, top-of-canopy (TOC) SIF has been retrieved at various scales and spatial resolutions using ground-based, airborne and satellite platforms [1]-[3]. SIF has largely been retrieved using leaf and ground-based canopy-level sensors, gradually scaling up to satellite platforms for global vegetation monitoring purposes. However, the intermediate scales provided by airborne platforms are critical to bridge the gap between field and satellite-based SIF observations and to disentangle the contribution by the different scene components in aggregated pixels [4], [5]. In this context, assessing the spectral configurations and spatial requirements for the operational use of SIF in precision agriculture and plant phenotyping trials is crucial.

The SR of the sensor is a critical factor that influences the accuracy of the quantified SIF. Modelling based studies [6], [7] have demonstrated that the use of broader-band sensors leads to a higher SIF retrieval bias from FLD-based approaches. As a result, very high-resolution imaging sensors are needed to quantify SIF in absolute terms accurately. Although broader-band sensors (e.g. in the range of 5-6 nm FWHM SR) are sub-optimal for the absolute quantification of SIF at the O_2-A feature, several studies have demonstrated that the relative SIF variability captured by such sensors is a valuable plant trait in the context of plant physiology, gross primary productivity monitoring and for the early detection of biotic and abiotic stress [2], [8]-[10]. Studies comparing SIF retrievals from narrow-band (i.e. below 1 nm FWHM) vs. broader-band hyperspectral imagers (ca. 5-6 nm FWHM) flown in tandem over experimental fields displaying a range of physiological condition are therefore needed. This study aims to evaluate the SIF quantification from broader-band vs. sub-nanometer airborne imagers for stress detection and assessment of crop physiological conditions.

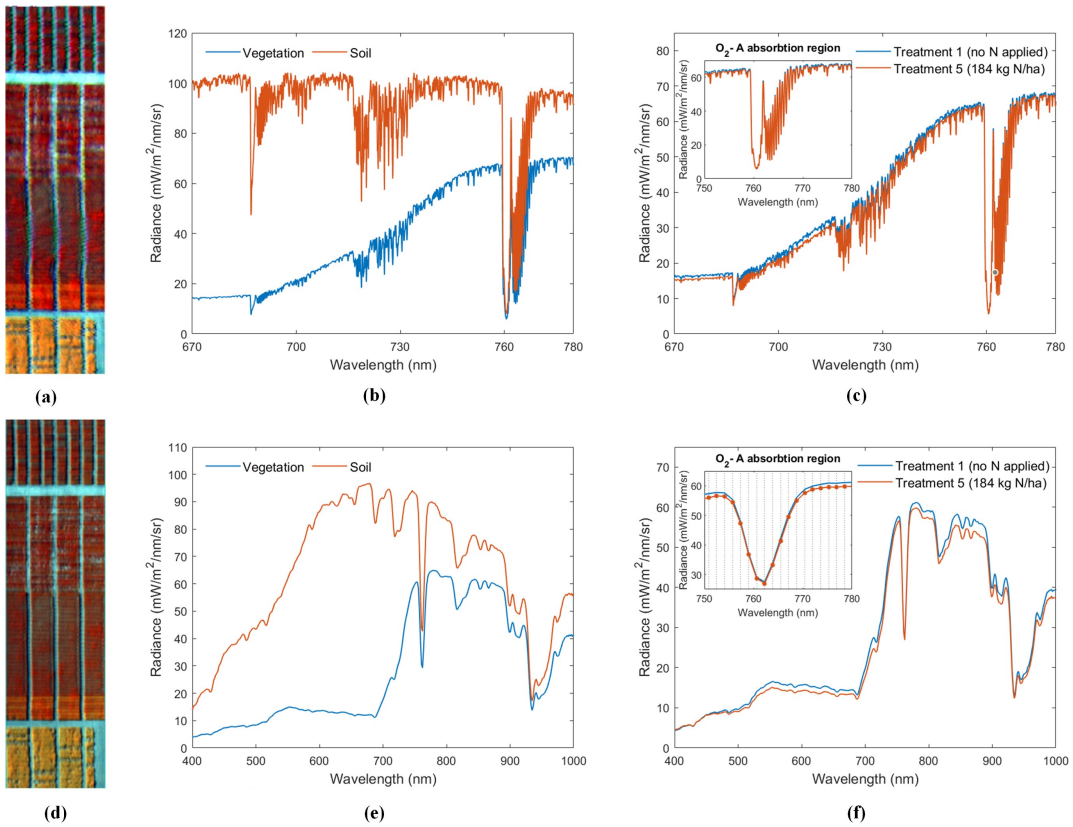

Fig. 1: Subset of the imagery acquired from the aircraft yielding 20 cm pixel resolution and the corresponding sample radiance spectra from the narrow-band hyperspectral imager (a; b) and from the broader-band hyperspectral imager (d; e). Comparison of the radiance spectra for treatment 1 plot with no N applied vs. treatment 5 with the highest levels of N applied (184 kg N/ha) extracted from the narrow-band (c) and broader-band imagers (f). The vertical lines in (f) indicate the location of the 18 spectral bands within the O_2-A absorption region for SIF quantification with the broader-band hyperspectral imager.

2. MATERIALS AND METHODS

2.1. Study sites, field experiment and airborne campaign

The experiment was conducted over fifteen dryland wheat (cv. Scepter) [11] plots located at Yarrawonga, Victoria, Australia. The 2 m × 13 m plots were planted in May 2019 and treated with five different nitrogen (N) application rates in the form of Urea (46% N) fertilizer (T1: 0 kg N/ha, T2: 46 kg N/ha, T3: 92 kg N/ha, T4: 138 kg N/ha, T5: 184 kg N/ha). Leaf-level measurements of steady-state chlorophyll fluorescence (F_t) were performed in the field on ten leaves per plot using the FluorPen device (PSI, Czech Republic) at the time of the airborne campaign.

The airborne campaign to collect TOC spectral radiances was carried out under clear sky conditions on 9 October 2019 from 15:40 to 16:30 local time flying with the heading of the aircraft on the solar plane. The payload consisted of two hyperspectral imagers installed in tandem on a Cessna aircraft operated by the HyperSens Laboratory, University of Melbourne's Airborne Remote Sensing Facility. The first linear-array hyperspectral camera used in this study was the Micro-Hyperspec VNIR E-Series model (Headwall Photonics, Fitchburg, MA, USA) operated with a configuration of 371 spectral bands acquired at 1.626 nm/pixel in the 400–1000 nm region, yielding 5.8 nm FWHM. The second hyperspectral camera was the high-resolution chlorophyll fluorescence imager (Headwall Photonics, Fitchburg, MA, USA) operated with a configuration of 2160 spectral bands acquired at 0.051 nm/pixel in the 670–780 nm region, yielding 0.1-0.2 nm FWHM. Fig. 1 shows a portion of the imagery along with sample radiance spectra acquired from both imagers. Differences in the radiance spectra and the O_2-A feature were visually detected as a function of the nitrogen rates applied over the experimental fields (Fig. 1c and Fig. 1f).

2.2. SIF quantification from field data and airborne hyperspectral imagery

The mean radiance spectra from each plot were calculated by computing the average of all pixels within each region of interest, excluding the boundaries and non-vegetation pixels. The total incoming irradiance at the time of the flight was measured using a 0.065 nm FWHM Ocean Optics HR2000 fiber-optics spectrometer (Ocean Optics, Dunedin, FL,

USA) with a CC-3 VIS-NIR cosine corrector diffuser (Ocean Optics, Dunedin, FL, USA).

The radiometric calibration of the spectrometer was carried out using the coefficients derived from a uniform calibrated light source and an integrating sphere (model XTH2000C, Labsphere Inc., North Sutton, NH, USA) using six different levels of illumination. To match the spectral resolution of the radiance images acquired from both imagers, the high-resolution irradiance spectra collected with the HR2000 spectrometer was resampled through Gaussian convolution corresponding to the spectral resolution of the airborne imagers. The SIF quantification from both instruments was conducted using the O_2-A band *in-filling* method through the FLD principle [12], using a total of three spectral bands (3FLD) [13]. SIF was scaled based on an offset derived from non-fluorescence targets extracted from the imagery to account for the effects of negative values due to atmospheric and calibration factors. In addition to the SIF quantification through the 3FLD method, the depth at the O_2-A absorption feature captured by the two imagers was also quantified.

3. RESULTS

The different spectral characteristics of the two hyperspectral imagers caused significant effects in the measured radiances (Fig. 2). As expected, the depth and shape of the absorption features at the O_2-A (760.4 nm) and O_2-B (687.0 nm) were strongly influenced by the SR. The O_2-B absorption feature could not be identified in the broader-band radiance spectra. A reduction in the O_2-A band depth and an increase in the radiance signal of the absorption minimum were also observed. As reported in other studies, the wavelength corresponding to the radiance minimum was shifted towards higher wavelengths when compared to the narrow-band imager.

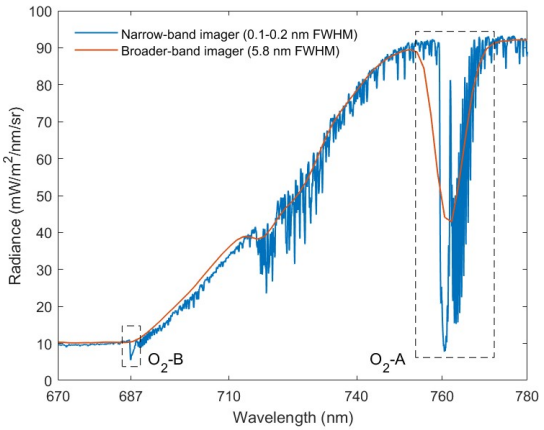

Fig. 2: Comparison of radiance spectra acquired from the narrow-band and broader-band airborne hyperspectral imagers for the same experimental plot.

The O_2-A absorption band depth calculated from the two hyperspectral imagers from radiance spectra extracted from the experimental plots with nitrogen variability exhibited a strong relationship (R^2=0.84, $p<0.001$; Fig. 3a). Results obtained when comparing SIF quantified through 3FLD from the two airborne hyperspectral imagers is illustrated in Fig 3b. As the retrieval of SIF at O_2-A band using the FLD principle is primarily affected by the depth of the measured O_2-A absorption feature (shown in Fig. 2 & 3a), large differences in the range of SIF levels from both imagers as a function of the spectral resolution were observed. Although in absolute terms the SIF levels were affected by the spectral resolution of both imagers (RMSE=3.7 mW/m^2/nm/sr), a significant relationship was obtained (R^2=0.71, $p<0.001$) which demonstrates the agreement in the relative variability of SIF quantified by the two imagers at the O_2-A feature.

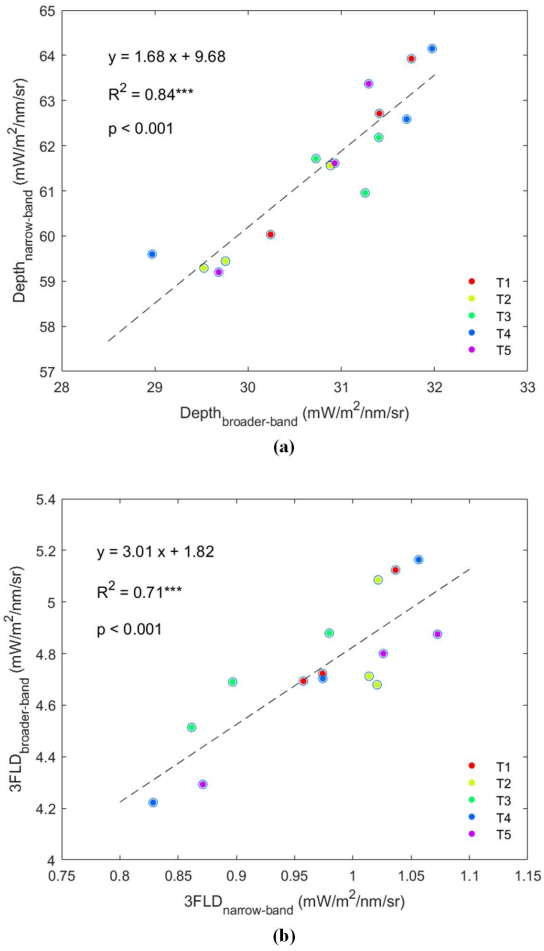

Fig. 3: Relationship between O_2-A band depth captured by the two imagers (a). Relationship between the airborne SIF quantified using the 3FLD method from the two imagers (b).

The assessment of the TOC airborne SIF quantified by both imagers was conducted by comparing against fluorescence measurements carried out at the leaf-level

across the experimental field. The relationships obtained between leaf-level fluorescence and airborne SIF yielded significant results (R^2=0.65, p<0.001 for the narrow-band imager, and R^2=0.42, p<0.01 for broader-band imager).

Our results demonstrate the link between the airborne-retrieved SIF from two hyperspectral imagers with different spectral resolutions. These results obtained by sensors flying in tandem support the findings of past studies [2], [9], [10] that showed the capability of broader-band hyperspectral imagers for SIF quantification in the context of early detection of vegetation stress symptoms and plant physiological assessment.

4. CONCLUSIONS

This study assessed the effects of varying spectral resolution from two airborne hyperspectral imagers on the quantification of SIF at the O_2-A absorption feature for vegetation stress detection and plant phenotyping purposes when flown over experimental wheat plots with variable nitrogen rates. The airborne hyperspectral images acquired at 20 cm spatial resolution from a sub-nanometer (0.1-0.2 nm FWHM) and a broader-band imager (5.8 nm FWHM) flown in tandem yielded a bias (RMSE=3.7 mW/m^2/nm/sr) in the absolute SIF levels quantified by both imagers, but a good agreement when comparing the O_2-A feature depth (R^2=0.84) and the 3FLD quantification (R^2=0.71). These results demonstrate the potentials of using broader-band hyperspectral imagers for operational retrievals of SIF in the context of plant phenotyping and precision agriculture, where quantification of relative stress levels is required. This study also makes progress toward future work to model the effect of sensor spectral resolution on the retrieved SIF from piloted and drone-based airborne hyperspectral imagers for vegetation stress detection.

5. ACKNOWLEDGEMENTS

The authors gratefully acknowledge the Foundation for Arable Research Australia and Riverine Plains Incorporated for their provision and management of the plot trials. A. Gracia-Romero is acknowledged for his technical support during the field and airborne campaigns.

6. REFERENCES

[1] O. Pérez-Priego, P.J. Zarco-Tejada, J.R. Miller, G. Sepulcre-Cantó, and E. Fereres, "Detection of water stress in orchard trees with a high-resolution spectrometer through chlorophyll fluorescence *in-filling* of the O_2-A band," *IEEE Trans. Geosci. Remote Sens.*, vol. 43, no. 12, pp. 2860–2868, Dec. 2005.

[2] P.J. Zarco-Tejada, M.V. González-Dugo, and E. Fereres, "Seasonal stability of chlorophyll fluorescence quantified from airborne hyperspectral imagery as an indicator of net photosynthesis in the context of precision agriculture," *Remote Sens. Environ.*, vol. 179, pp. 89–103, Jun. 2016.

[3] J. Joiner, Y. Yoshida, A. P. Vasilkov, Y. Yoshida, L. A. Corp, and E. M. Middleton, "First observations of global and seasonal terrestrial chlorophyll fluorescence from space," *Biogeosciences*, vol. 8, no. 3, pp. 637–651, 2011.

[4] P. J. Zarco-Tejada, L. Suarez, and V. Gonzalez-Dugo, "Spatial resolution effects on chlorophyll fluorescence retrieval in a heterogeneous canopy using hyperspectral imagery and radiative transfer simulation," *IEEE Geosci. Remote Sens. Lett.*, vol. 10, no. 4, pp. 937–941, Jul. 2013.

[5] A. Hornero et al., "Assessing the contribution of understory sun-induced chlorophyll fluorescence through 3-D radiative transfer modelling and field data," *Remote Sens. Environ*., vol. 253, Feb. 2021

[6] A. Damm et al., "Modeling the impact of spectral sensor configurations on the FLD retrieval accuracy of sun-induced chlorophyll fluorescence," *Remote Sens. Environ.*, vol. 115, no. 8, pp. 1882–1892, Aug. 2011.

[7] L. Liu, X. Liu, and J. Hu, "Effects of spectral resolution and SNR on the vegetation solar-induced fluorescence retrieval using FLD-based methods at canopy level," *Eur. J. Remote. Sens.*, vol. 48, pp. 743–762, 2015.

[8] A. Damm, L. Guanter, V. C. E. Laurent, M. E. Schaepman, A. Schickling, and U. Rascher, "FLD-based retrieval of sun-induced chlorophyll fluorescence from medium spectral resolution airborne spectroscopy data," *Remote Sens. Environ.*, vol. 147, pp. 256–266, May 2014.

[9] A. Damm et al., "Far-red sun-induced chlorophyll fluorescence shows ecosystem-specific relationships to gross primary production: An assessment based on observational and modeling approaches," *Remote Sens. Environ.*, vol. 166, pp. 91–105, Sep. 2015.

[10] P. J. Zarco-Tejada et al., "Previsual symptoms of *Xylella fastidiosa* infection revealed in spectral plant-trait alterations," *Nat. Plants*, vol. 4, no. 7, pp. 432–439, Jul. 2018.

[11] R. Yang et al., "Molecular characterisation of the NAM-1 genes in bread wheat in Australia," *Crop and Pasture Science*, vol. 69, no. 12, pp. 1173–1181, 2018.

[12] J. A. Plascyk and F. C. Gabriel, "The Fraunhofer Line Discriminator MKII-An Airborne Instrument for Precise and Standardized Ecological Luminescence Measurement," *IEEE Trans. Instrum. Meas.*, vol. 24, no. 4, pp. 306–313, Dec. 1975.

[13] S. W. Maier, K. P. Gunther, and M. Stellmes, "Sun-Induced Fluorescence: A New Tool for Precision Farming," In: *Digital Imaging and Spectral Techniques: Applications to Precision Agriculture and Crop Physiology*, Vol. 66 (eds M McDonald, J Schepers, L Tartly, T Van Toai, D Major), ASA Spec. Publ., Madison, WI, USA, pp. 209– 222, 2003.